

# Asymmetric deceleration of ClpB or Hsp104 ATPase activity unleashes protein-remodeling activity

Shannon M Doyle<sup>1,4</sup>, James Shorter<sup>2,4</sup>, Michal Zolkiewski<sup>3</sup>, Joel R Hoskins<sup>1</sup>, Susan Lindquist<sup>2</sup> & Sue Wickner<sup>1</sup>

**Two members of the AAA+ superfamily, ClpB and Hsp104, collaborate with Hsp70 and Hsp40 to rescue aggregated proteins. However, the mechanisms that elicit and underlie their protein-remodeling activities remain unclear. We report that for both Hsp104 and ClpB, mixtures of ATP and ATP- $\gamma$ S unexpectedly unleash activation, disaggregation and unfolding activities independent of cochaperones. Mutations reveal how remodeling activities are elicited by impaired hydrolysis at individual nucleotide-binding domains. However, for some substrates, mixtures of ATP and ATP- $\gamma$ S abolish remodeling, whereas for others, ATP binding without hydrolysis is sufficient. Remodeling of different substrates necessitates a diverse balance of polypeptide 'holding' (which requires ATP binding but not hydrolysis) and unfolding (which requires ATP hydrolysis). We suggest that this versatility in reaction mechanism enables ClpB and Hsp104 to reactivate the entire aggregated proteome after stress and enables Hsp104 to control prion inheritance.**

Life demands that members of the 'ATPases associated with various cellular activities' (AAA+) superfamily couple energy from ATP hydrolysis to the remodeling of a bewildering array of macromolecular structures, ranging from protein to DNA and RNA<sup>1,2</sup>. Typically, eukaryotic genomes encode 50–80 family members<sup>1</sup>, each of which occupies specific niches that require specialized modes of substrate selection and regulation. The extraordinary adaptive radiation of AAA+ proteins to function in a multitude of cellular reactions demonstrates the versatility of their structurally conserved AAA+ domain. Subunits containing AAA+ domains assemble into oligomeric rings, and ATP binds at the interface between adjacent protomers<sup>1,2</sup>. AAA+ oligomers undergo considerable conformational changes during ATP binding and hydrolysis, although how these events are regulated and transduced into productive substrate remodeling remains largely enigmatic. Furthermore, it remains unanswered whether individual AAA+ family members rely on a common reaction mechanism to remodel various macromolecular clients. It is also unclear whether different AAA+ members have evolved distinct methods to engage and restructure substrates, or whether individual proteins can switch between distinct reaction mechanisms for different substrates.

Two members of the AAA+ superfamily separated by ~2 billion years of evolution<sup>3</sup>, yeast Hsp104 and its *Escherichia coli* homolog, ClpB, allow cell survival after exposure to extreme environmental stress<sup>4–7</sup>. They function to dissolve and renature thousands of diverse substrates during reactivation of the aggregated proteome after multifarious stresses. They work in collaboration with the Hsp70/DnaK chaperone system<sup>8–10</sup>, and as a result, cell survival can increase by

10,000-fold<sup>4–7</sup>. Under normal growth conditions, Hsp104 is also essential for the formation and maintenance of prions, protein-based genetic elements comprised of amyloid fibers that self-perpetuate changes in protein conformation and function<sup>11</sup>.

How does the structure of ClpB and Hsp104 facilitate these functions? Both are hexamers comprised of protomers containing two AAA+ ATPase domains (nucleotide-binding domains 1 and 2, NBD-1 and NBD-2) and an N-terminal domain<sup>12</sup> (Fig. 1a). Inserted in NBD-1 is a long coiled-coil middle domain that resembles in structure the shape of a two-bladed propeller<sup>12</sup> and distinguishes ClpB and Hsp104 from other Hsp100 proteins that also contain two NBDs<sup>1</sup>. Electron microscopy and single-particle reconstruction of Hsp104 and ClpB reveal an axial channel spanning the length of the hexamer<sup>13,14</sup>. Although not completely visible, the coiled-coil middle domains are proposed to be located on the outside of the ClpB hexamer<sup>12</sup>. ATP is bound at the interface between adjacent subunits<sup>12</sup> and hexamerization is stabilized by nucleotide<sup>13,14</sup>. Substrate binding occurs when the hexamer is in its ATP-bound conformation and conserved pore residues may contact substrates directly<sup>15–17</sup>. The N- and C-terminal domains may also help engage substrates and cofactors<sup>18,19</sup>. Cooperative ATPase activity occurs at both NBD-1 and NBD-2, and allosteric communication occurs within and between the two domains<sup>12,19–23</sup>. Disruption of ATPase activity and consequent inhibition of conformational changes compromises protein-remodeling activity<sup>15–17,19,21</sup>. However, despite intense investigation, it remains unclear how the hexameric architecture of ClpB and Hsp104 contributes to the conformational changes associated with the dissolution and reactivation of aggregated proteins<sup>24</sup>.

<sup>1</sup>Laboratory of Molecular Biology, National Cancer Institute, National Institutes of Health (NIH), Bethesda, Maryland 20892, USA. <sup>2</sup>Whitehead Institute for Biomedical Research, Nine Cambridge Center, Cambridge, Massachusetts 02142, USA. <sup>3</sup>Department of Biochemistry, Kansas State University, Manhattan, Kansas 66506, USA. <sup>4</sup>These authors contributed equally to this work. Correspondence should be addressed to S.W. (wickners@mail.nih.gov) or S.L. (lindquist\_admin@wi.mit.edu).

Received 2 October 2006; accepted 2 January 2007; published online 28 January 2007; doi:10.1038/nsmb1198

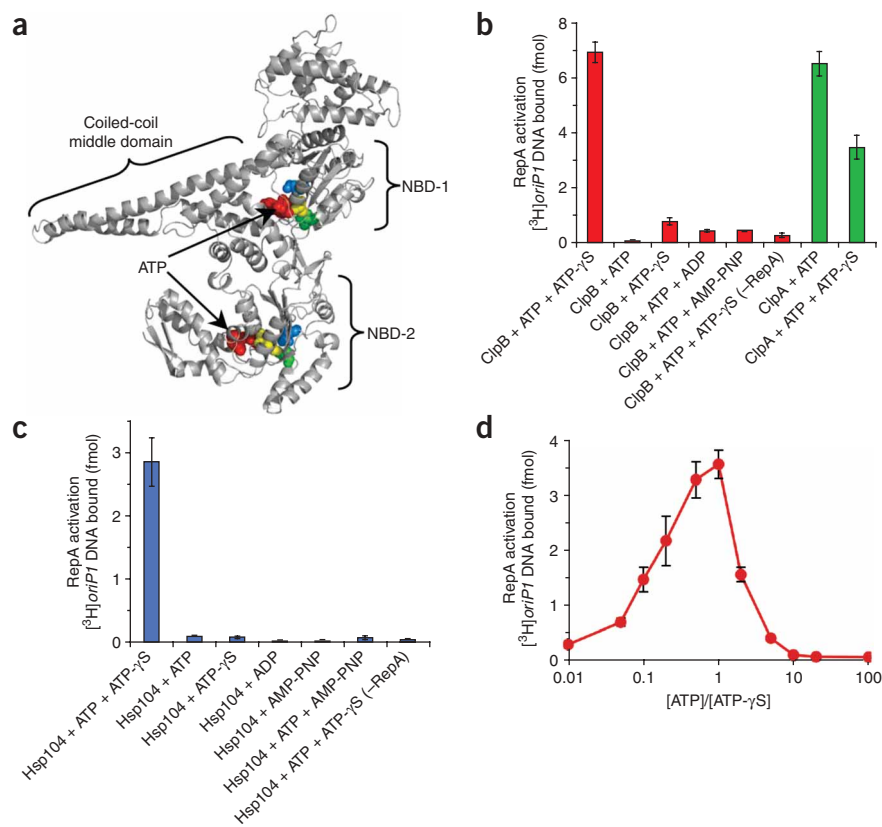


**Figure 1** Protein activation by ClpB or Hsp104 alone. (a) Model of *E. coli* ClpB subunit. Each monomer has two nucleotide-binding domains, NBD-1 and NBD-2, which are separated by a large coiled-coil middle domain. Within each NBD is a Walker A, a Walker B and a sensor-1 motif. CPK models show positions of ATP (red), Lys212 and Lys611 of Walker A motif (yellow), Glu279 and Glu678 of Walker B motif (blue) and Thr315 and Asn719 of sensor-1 motif (green). Model was generated using Swiss-Model<sup>53</sup> and based on the crystal structure of *Thermus thermophilus* ClpB<sup>12</sup>. (b) RepA activation by ClpB or ClpA. (c) RepA activation by Hsp104. (d) RepA activation by ClpB with varying ratios of ATP to ATP-γS. In **b–d**, data are means ± s.d. (*n* = 3).

## RESULTS

### Protein remodeling by ClpB and Hsp104 without cochaperones

We sought conditions that might activate the remodeling activities of ClpB in the absence of cochaperones. As a model substrate, we began with inactive dimers of RepA, a protein that initiates the replication of P1 plasmids in *E. coli*. RepA dimers are converted by either the Hsp70/DnaK chaperone system or by ClpA into active monomers that bind the plasmid replication origin, *oriP1*, with high affinity<sup>29,30</sup>. ClpB had no capacity to activate RepA in the presence of ATP (Fig. 1b). To

our surprise, a 1:1 mixture of ATP and ATP-γS greatly stimulated RepA activation by ClpB (Fig. 1b). ATP-γS alone did not support remodeling (Fig. 1b).

Hsp104 also activated RepA when provided a mixture of ATP and ATP-γS (Fig. 1c). As with ClpB, neither ATP nor ATP-γS alone supported activation (Fig. 1c). The optimal ATP/ATP-γS ratio was 1:1 for ClpB activity (Fig. 1d) and 3:1 for Hsp104 activity (data not shown). Moreover, a mixture of ATP with ADP or of ATP with AMP-PNP (a nonhydrolyzable ATP analog) did not support the remodeling reaction (Fig. 1b). ClpA, another hexameric AAA+ ATPase with two AAA+ domains per monomer, but which lacks the coiled-coil middle domain present in Hsp104 and ClpB (Fig. 1a), behaved differently. ClpA activated RepA in the presence of ATP alone<sup>29</sup> and a mixture of ATP with ATP-γS was inhibitory (Fig. 1b). These results show that the remodeling activity of ClpB and Hsp104 is elicited by a combination of ATP and ATP-γS. Although ATP-γS is known to inhibit ATP hydrolysis, slowing hydrolysis of ATP is not its function here, as AMP-PNP and ADP, which are also expected to reduce ATP hydrolysis, were ineffective.

### Protein disaggregation by ClpB and Hsp104

The observation that ClpB and Hsp104 have innate chaperone activity allowed us to examine, for the first time, the remodeling activity of these proteins without cochaperones. We began by asking whether mixtures of ATP and ATP-γS also elicit the disaggregation of larger aggregates by ClpB or Hsp104. We used thermally denatured green fluorescent protein (GFP) aggregates ~500 kDa or greater in size<sup>31</sup> as a substrate. Remarkably, both ClpB (Fig. 2a) and Hsp104 (Fig. 2b) promoted reactivation of heat-aggregated GFP in the presence of ATP and ATP-γS.

The powerful remodeling activities of Hsp104 and ClpB must be tightly regulated and highly discriminating, because even very high levels of expression are not toxic<sup>5,25</sup>. That is, despite a capacity to engage diverse substrates, ClpB and Hsp104 do not interfere with large functional protein complexes or filamentous structures. Most notably, a screen for mutations that perturb the regulated function of Hsp104 has revealed that single-amino acid substitutions in an NBD combined with single-amino acid substitutions in the coiled-coil middle domain frequently cause Hsp104 to become highly toxic<sup>25</sup>. This suggests that the tight regulation of ClpB and Hsp104 may stem, in part, from the intrinsic properties of the hexamer itself. However, a clear understanding of how Hsp104 and ClpB are tightly regulated remains elusive.

In this study, we investigated the innate protein-remodeling activity of yeast Hsp104 and *E. coli* ClpB. We establish the unexpected ability of mixtures of ATP and ATP-γS (a nonphysiological and slowly hydrolyzed ATP analog) to elicit Hsp104 and ClpB activity in protein activation, disaggregation and unfolding assays. Notably, the functions of Hsp104 and ClpB were elicited without assistance from cochaperones. Thus far, ClpB has been observed to require Hsp70/DnaK and Hsp40/DnaJ for every protein-remodeling activity tested<sup>9,10</sup>. Previously, Hsp104 has been observed to remodel only yeast prion proteins independently of cochaperones<sup>26,27</sup>. Hsp104 also reactivates some protein aggregates with the assistance of the small heat-shock protein Hsp26 (ref. 28). However, with most substrates, Hsp104 requires Hsp70 and Hsp40 chaperones<sup>8</sup>. Hence, the effect of mixtures of ATP and ATP-γS allowed us to study ClpB and Hsp104 remodeling activities without any confounding effects of cochaperones. Our findings bring significant new insights into the mechanistic basis by which Hsp104 and ClpB hexamers function and elucidate the coordinated roles of the two AAA+ domains in protein remodeling.

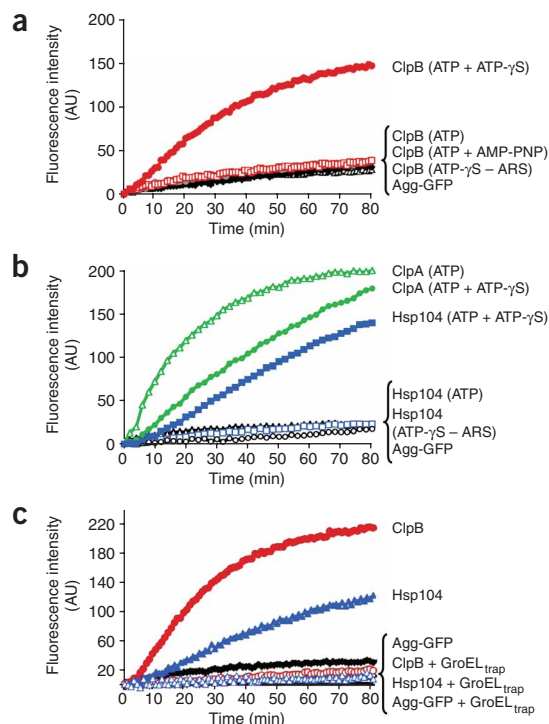


**Figure 2** Reactivation of heat-aggregated proteins by ClpB or Hsp104 alone. (a) Disaggregation of heat-aggregated GFP by ClpB. –ARS, absence of ATP-regeneration system; Agg-GFP, aggregated GFP alone. (b) Disaggregation of aggregated GFP by Hsp104 or ClpA. (c) Disaggregation and release of unfolded GFP by ClpB or Hsp104. In a–c, the initial fluorescence was set equal to 0 and a data set representative of three or more replicates is shown. AU, arbitrary units.

Activation of ClpB and Hsp104 by mixtures of ATP and ATP-γS was highly specific. ATP or ATP-γS alone did not support disaggregation by ClpB or Hsp104 and neither did a mixture of ATP and AMP-PNP or a mixture of ATP and ADP (Fig. 2a,b and data not shown). ClpA also reactivated aggregated GFP, an activity of ClpA not previously observed. In contrast to Hsp104 and ClpB, ClpA required ATP and the addition of ATP-γS was inhibitory (Fig. 2b). Thus, for ~2 billion years of evolution<sup>3</sup>, a distinct mechanism for unleashing the protein-remodeling activities of the ClpB/Hsp104 class of proteins—a mechanism which is mimicked *in vitro* by the mixture of ATP and ATP-γS—has been conserved.

### Release of unfolded polypeptides during disaggregation

The unexpected stimulation of ClpB and Hsp104 disaggregation activity by the mixture of ATP and ATP-γS led us to investigate the nature of the disaggregation reaction products. To do so, we used a mutant chaperonin, GroEL<sub>trap</sub> (ref. 32) that captures unfolded proteins in the molten-globule state<sup>33</sup> and prevents refolding but does not bind heat-aggregated GFP<sup>31</sup> or native GFP<sup>32</sup>. GroEL<sub>trap</sub> inhibited reactivation of aggregated GFP by Hsp104 and ClpB (Fig. 2c). Thus, Hsp104 and ClpB release GFP in an unfolded state that can be captured by GroEL<sub>trap</sub>.

### ClpB and Hsp104 can unfold native protein structures

ClpB and Hsp104 have never been found to unfold native proteins. Might the combination of ATP and ATP-γS elicit such an activity?

To test this, we used GFP as our substrate, because it is extremely stable ( $T_m \sim 70^\circ\text{C}$ ) and can withstand mechanical unfolding forces of ~100 pN (ref. 34). As GFP refolds rapidly once unfolded, we used GroEL<sub>trap</sub> to capture potential unfolded products. However, native GFP was not unfolded by ClpB or Hsp104 (data not shown). We then tested a GFP fusion protein containing a fragment of RepA (amino acid residues 1–70) to provide a possible recognition signal. With both ClpB and Hsp104, a large loss of GFP fluorescence occurred when RepA<sub>1–70</sub>-GFP was incubated with a mixture of ATP and ATP-γS in the presence of GroEL<sub>trap</sub> (Fig. 3a,b). Thus, some feature of the RepA<sub>1–70</sub> fragment, probably the unstructured N-terminal end, provides a recognition signal for substrate engagement and allows ClpB and Hsp104 to unfold even highly stable proteins.

Again, the effect of ATP and ATP-γS mixtures was specific. No unfolding occurred when ClpB or Hsp104 were incubated with ATP-γS (Fig. 3a,b). Nor was RepA<sub>1–70</sub>-GFP unfolding observed when ClpB was incubated in the presence of ATP (Fig. 3b), and very little occurred with Hsp104 in the presence of ATP (Fig. 3a). Titrating ATP from 2 mM to 5 μM, in an effort to slow hydrolysis by limiting ATP, also did not promote unfolding by ClpB (data not shown). Mixtures of ATP and ADP, or ATP and AMP-PNP, also did not promote unfolding (data not shown). As with the activation and disaggregation reactions, the optimal ATP/ATP-γS ratio for ClpB was ~1:1 (data not shown). In contrast, ClpA catalyzed unfolding with ATP alone<sup>29</sup> and ATP-γS was inhibitory (Fig. 3a). Thus Hsp104 and ClpB utilize a different mechanism than ClpA to couple ATP hydrolysis to protein unfolding, although the end result of hydrolysis, unfolded substrate, is the same.

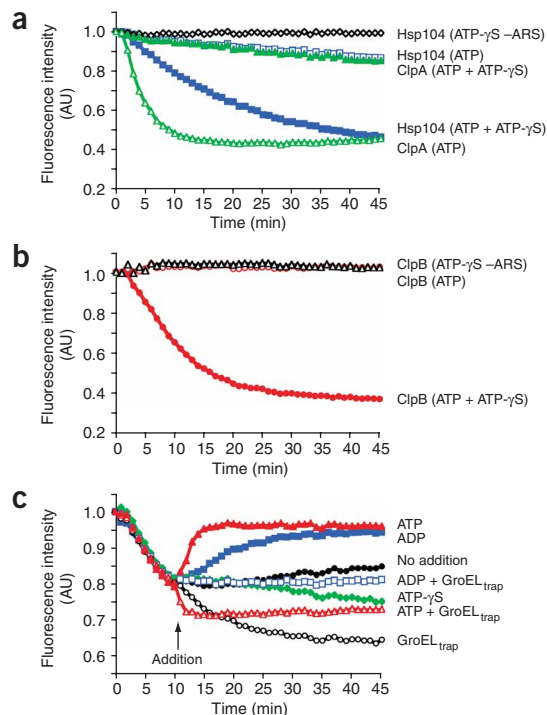
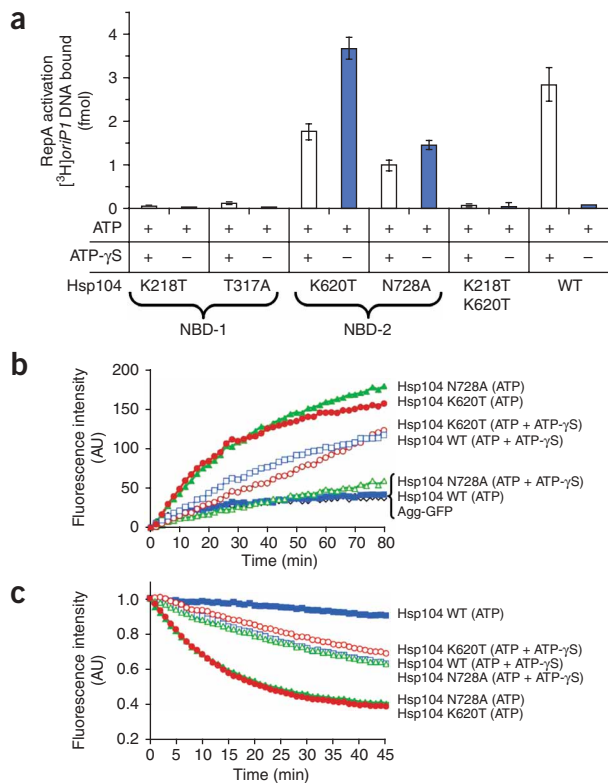


**Figure 3** Protein unfolding by ClpB or Hsp104 alone. (a) Unfolding of RepA<sub>1–70</sub>-GFP by Hsp104 or ClpA alone. (b) Unfolding of RepA<sub>1–70</sub>-GFP by ClpB. (c) Steady-state unfolding of RepA<sub>1–70</sub>-GFP by ClpB. At the time indicated, an excess of the component indicated was added. In a–c, the initial fluorescence was set equal to 1 and a data set representative of three or more replicates is shown. AU, arbitrary units.



### Mechanism of stimulation by mixtures of ATP and ATP- $\gamma$ S

To investigate the mechanism by which the combination of ATP and ATP- $\gamma$ S elicited ClpB remodeling activities, we sought to challenge a steady-state unfolding reaction with excess ATP, ATP- $\gamma$ S or ADP. First, we established that steady-state unfolding could be achieved in the presence of ATP and ATP- $\gamma$ S (Fig. 3c). When ClpB was incubated with both nucleotides in the absence of GroEL<sub>trap</sub>, a decline in RepA<sub>1-70</sub>-GFP fluorescence occurred, reaching a plateau after 10 min (Fig. 3c). This was due to a steady-state equilibrium between unfolding and refolding. Over the next 90 min, as the energy supply was exhausted, the rate of unfolding slowed and the fluorescence slowly returned to the original level (data not shown). If GroEL<sub>trap</sub> was added at 10 min to capture released unfolded products, fluorescence slowly declined (Fig. 3c).

The addition of excess ATP after 10 min caused an immediate increase in fluorescence, indicating that the replacement of ATP- $\gamma$ S with ATP in this steady-state reaction promotes substrate release (which is followed by spontaneous RepA<sub>1-70</sub>-GFP refolding) (Fig. 3c). When GroEL<sub>trap</sub> was added together with excess ATP, there was a rapid decrease in fluorescence followed by a plateau (Fig. 3c). This suggests that ATP does not simply trigger release of substrate but also produces a burst of substrate unfolding and release, as revealed by the capture of increased quantities of unfolded RepA<sub>1-70</sub>-GFP by GroEL<sub>trap</sub>. In contrast, the addition of excess ATP- $\gamma$ S was followed by a gradual decrease in fluorescence, with or without GroEL<sub>trap</sub>, indicating that slow hydrolysis increases the residence time of the substrate with ClpB (Fig. 3c and data not shown). The addition of excess ADP resulted in an increase in fluorescence, indicating substrate release followed by refolding (Fig. 3c). The addition of ADP with GroEL<sub>trap</sub>, unlike the addition of ATP with GroEL<sub>trap</sub>, stopped any further changes in fluorescence, revealing that substrate was released without additional unfolding (Fig. 3c). There-

**Figure 4** Protein remodeling by Hsp104 NBD mutants. (a) RepA activation by Hsp104 and its mutants in NBD-1 and NBD-2. Data are means  $\pm$  s.d. ( $n = 3$ ). WT, wild-type. (b) Reactivation of heat-aggregated GFP by Hsp104 mutants. The initial fluorescence was set equal to 0 and a data set representative of three or more replicates is shown. Agg-GFP, aggregated GFP alone; AU, arbitrary units. (c) Unfolding of RepA<sub>1-70</sub>-GFP by Hsp104 mutants. The initial fluorescence was set equal to 1 and a data set representative of three or more replicates is shown.

fore, ATP- $\gamma$ S promotes substrate ‘holding’, whereas ATP hydrolysis is required for substrate unfolding and release. These results suggest that the combination of ATP- $\gamma$ S with ATP unleashes ClpB remodeling activities by allowing ClpB hexamers to achieve a balance of substrate binding, holding and unfolding to forcibly unfold proteins.

### Roles of two AAA+ domains in Hsp104 substrate remodeling

To determine whether NBD-1, NBD-2 or both require restrained hydrolysis to promote substrate remodeling, we tested mutants with amino acid substitutions in each domain. We used Hsp104 mutants with a substitution in the Walker A box (a motif containing a lysine residue that directly contacts the phosphates of ATP<sup>1</sup>) of either NBD-1 or NBD-2 (Fig. 1a). The Walker A mutants are defective in ATP binding and thermotolerance<sup>35,36</sup>. We also analyzed mutants with a substitution in the sensor-1 motif (a motif containing a threonine or asparagine that interacts with the  $\gamma$ -phosphate of ATP<sup>1</sup>) of NBD-1 or NBD-2 (Fig. 1a). The sensor-1 mutants bind nucleotide, although they are defective in ATP hydrolysis and thermotolerance<sup>20</sup>.

Mutants with substitutions in NBD-2 of Hsp104, both in the Walker A (K620T) and sensor-1 (N728A) motifs, could activate RepA dimers (Fig. 4a), reactivate heat-aggregated GFP (Fig. 4b) and unfold RepA<sub>1-70</sub>-GFP (Fig. 4c). In all three reactions, the NBD-1 Walker A and sensor-1 mutants were inactive (Fig. 4a and data not shown). Furthermore, an Hsp104 mutant with both Walker A motifs mutated, Hsp104(K218T K620T)<sup>35</sup>, was also inactive (Fig. 4a and data not shown).

Notably, in contrast to wild-type Hsp104, the NBD-2 mutants used ATP as the sole nucleotide and ATP- $\gamma$ S was inhibitory (Fig. 4). These results indicate that remodeling of these substrates by Hsp104 is elicited when ATP hydrolysis is decelerated at NBD-2, but not at NBD-1. Deceleration of a subset of nucleotide-binding sites can be accomplished either through utilization of ATP- $\gamma$ S in combination with ATP or with mutants impaired in ATP hydrolysis at NBD-2.

### Roles of two AAA+ domains in ClpB substrate remodeling

There were differences between ClpB and Hsp104 in the involvement of the two NBDs, as might have been expected from the known functional differences in the NBDs of the two proteins. For example, NBD-1 of Hsp104 hydrolyzes ATP rapidly and is primarily involved in substrate binding, whereas NBD-2 hydrolyzes ATP much more slowly and is mainly responsible for oligomerization<sup>13,20,36</sup>. In contrast, NBD-1 and NBD-2 of ClpB hydrolyze ATP at similar rates and NBD-1 primarily contributes to oligomerization<sup>21,37,38</sup>.

We tested ClpB mutants comparable to the Hsp104 mutants described above, including mutants with substitutions in both Walker A motifs<sup>21,37</sup> that are known to be defective in ATP binding and thermotolerance as well as mutants with substitutions in both sensor-1 motifs (M. Barnett and M.Z., unpublished data) that can bind nucleotide, although they are defective in ATP hydrolysis and thermotolerance (Fig. 1a and Fig. 5). In addition, we tested mutants with substitutions in the ClpB Walker B box (a motif containing a catalytic



glutamate residue that activates a water molecule to hydrolyze ATP<sup>1</sup>) of NBD-1 or NBD-2 (Fig. 1a), which are defective in thermotolerance but bind and hydrolyze ATP<sup>21,39</sup>.

Like the Hsp104 NBD-2 mutants, the ClpB NBD-2 sensor-1 mutant (N719A) and the Walker B mutant (E678A) could activate RepA, reactivate heat-aggregated GFP and unfold RepA<sub>1-70</sub>-GFP (Fig. 5a,c,e). Notably, these ClpB mutants, like the Hsp104 NBD-2 mutants, used ATP as the sole nucleotide (Fig. 5a,c,e). ATP- $\gamma$ S inhibited activation, disaggregation and protein unfolding by the Walker B mutant and reactivation and protein unfolding by the sensor-1 mutant, although it did not inhibit RepA activation by the sensor-1 mutant (Fig. 5a,c,e). In contrast to Hsp104, the ClpB NBD-2 Walker A mutant (K611T) was inactive in all assays (Fig. 5a and data not shown). These data indicate that, as for Hsp104, deceleration of the ATPase activity at NBD-2 of ClpB, when NBD-1 remains active, can activate diverse protein-remodeling activities.

ClpB NBD-1 mutants differed from those of Hsp104. The NBD-1 sensor-1 mutant (T315A) and the Walker B mutant (E279A) were functional in activation, disaggregation and protein unfolding (Fig. 5a,b,d). In all cases, the ClpB Walker B mutant used ATP alone and ATP- $\gamma$ S was inhibitory (Fig. 5a,b,d). The ClpB NBD-1 sensor-1 mutant had substantially reduced activity compared to wild-type protein and used mixtures of ATP and ATP- $\gamma$ S more efficiently than ATP (Fig. 5a,b,d). A Walker A mutant in NBD-1 (K212T), like the analogous Hsp104 mutant, was inactive in all remodeling reactions with ATP and ATP- $\gamma$ S or ATP (Fig. 5a and data not shown). These data indicate that, unlike for Hsp104, deceleration of ClpB ATPase activity at NBD-1, when NBD-2 remains active, can also elicit protein-remodeling activity.

A ClpB double mutant in the Walker B motifs of NBD-1 and NBD-2 (E279A E678A)<sup>39</sup> was also inactive (Fig. 5a and data not shown). The inactivity of both ClpB(E279A E678A) and Hsp104(K218T K620T) indicates that deceleration of ATPase activity at NBD-2 can be counterproductive if NBD-1 also has no ATPase activity. Notably, together with the Hsp104 results, these experiments demonstrate a fundamental similarity in the mechanisms of Hsp104 and ClpB remodeling activities that we did not expect. Both proteins have an intrinsic capacity to remodel substrates in the absence of cochaperones, and this activity can be unleashed by blocking hydrolysis with mutations in a single AAA+ domain.

### Nucleotide hydrolysis by Hsp104 and ClpB

Next, we directly measured nucleotide hydrolysis by Hsp104 and ClpB using conditions where protein unfolding was apparent. Notably, mixtures of ATP and ATP- $\gamma$ S did not inhibit nucleotide hydrolysis, as would be expected for competition by a poorly hydrolyzable ATP analog. Instead, ATP- $\gamma$ S stimulated nucleotide hydrolysis by ClpB about three-fold in the presence of a 1:1 mixture of ATP and ATP- $\gamma$ S (Fig. 6a). To our surprise, nucleotide hydrolysis by ClpB with a 9:1

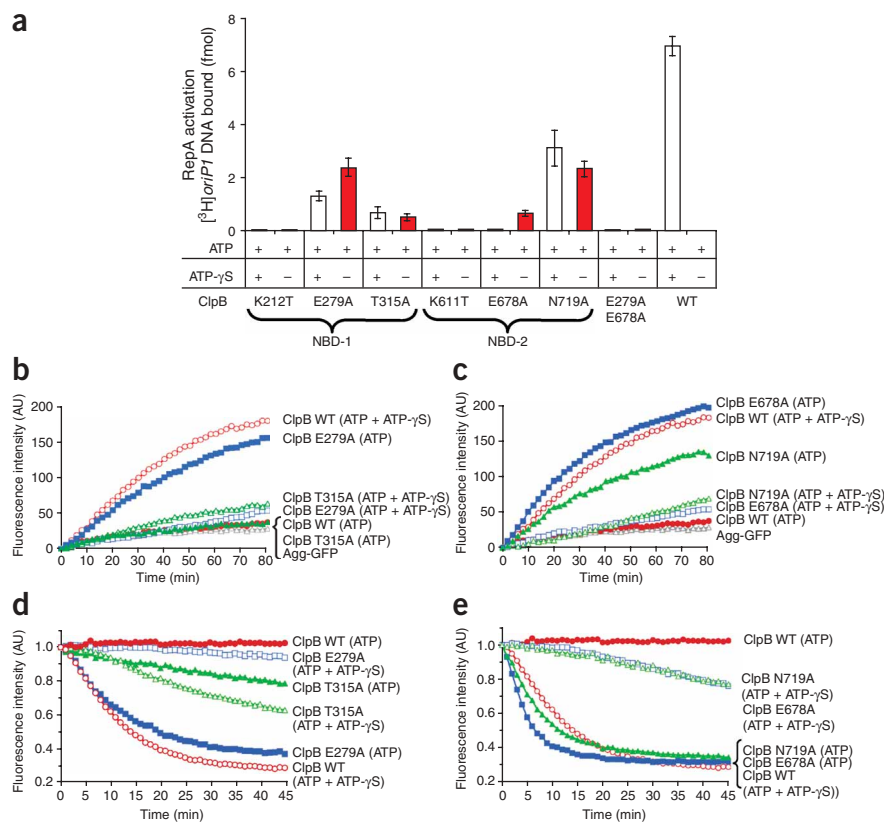


**Figure 5** Protein remodeling by ClpB NBD mutants. (a) RepA activation by ClpB mutants in NBD-1 and NBD-2. Data are means  $\pm$  s.d. ( $n = 3$ ). WT, wild-type. (b,c) Disaggregation of heat-aggregated GFP by ClpB NBD-1 (b) or NBD-2 (c) mutants. Initial fluorescence was set equal to 0 and a data set representative of three or more replicates is shown. Agg-GFP, aggregated GFP alone; AU, arbitrary units. (d,e) Unfolding of RepA<sub>1-70</sub>-GFP by ClpB NBD-1 (d) or NBD-2 (e) mutants. Initial fluorescence was set equal to 1 and a data set representative of three or more replicates is shown.

mixture of ATP- $\gamma$ S to ATP was approximately equal to that with ATP alone (Fig. 6a). Higher ratios of ATP- $\gamma$ S to ATP eventually became inhibitory (Fig. 6a). ATP- $\gamma$ S showed the predicted effect on nucleotide hydrolysis by ClpA: it was inhibitory at all ratios of ATP to ATP- $\gamma$ S (Fig. 6a). The unfolding substrate RepA<sub>1-70</sub>-GFP had a small inhibitory effect on nucleotide hydrolysis, and the activation substrate RepA had no effect (Fig. 6a and data not shown). These data unexpectedly demonstrate that ATP- $\gamma$ S stimulates nucleotide hydrolysis by ClpB.

To demonstrate whether ATP- $\gamma$ S stimulated hydrolysis of ATP or was itself hydrolyzed, we separately measured ATP and ATP- $\gamma$ S hydrolysis by ClpB using radiolabeled nucleotides. The rate of ClpB ATP hydrolysis increased about three-fold when the nucleotide source was a 1:1 mixture of ATP and ATP- $\gamma$ S, compared with the rate with ATP alone. The rate of ATP hydrolysis in the mixture (Fig. 6b) was similar to that of total nucleotide hydrolysis (Fig. 6a). The rate of ATP- $\gamma$ S hydrolysis by ClpB was 30-fold slower than that of ATP and was inhibited further when in a 1:1 mixture with ATP (Fig. 6b). Thus, ATP- $\gamma$ S specifically stimulated ATP hydrolysis by ClpB.

ATP hydrolysis by Hsp104 was not stimulated by ATP- $\gamma$ S at ratios of ATP to ATP- $\gamma$ S that activated remodeling, although it was not inhibited (Fig. 6c). The unfolding substrate RepA<sub>1-70</sub>-GFP did not appreciably affect the rate of ATP hydrolysis by Hsp104 in the absence or presence of ATP- $\gamma$ S (Fig. 6c). Thus, for both Hsp104 and ClpB, the effect of ATP- $\gamma$ S on ATP hydrolysis is a direct effect on ClpB or

Hsp104 and is independent of interactions of the substrate with ClpB or Hsp104.

For Hsp104, as for ClpB, the rate of ATP- $\gamma$ S hydrolysis was much slower than that of ATP and was inhibited further in a mixture of ATP- $\gamma$ S with ATP (Fig. 6c). Together, these results suggest that the binding or very slow hydrolysis of ATP- $\gamma$ S at some of the 12 ATP-binding sites of Hsp104 or ClpB may stimulate ATP hydrolysis at other sites by a mechanism of allosteric regulation that relieves the negative cooperativity in ATP hydrolysis. Thus, as is often the case with perturbations caused by drugs and mutations, the nonphysiological nucleotide ATP- $\gamma$ S revealed an aspect of the reaction mechanism for these proteins that would otherwise have remained undiscovered.

We also measured nucleotide hydrolysis by ClpB and Hsp104 mutants that are active in protein remodeling in the presence of ATP and are inhibited by mixtures of ATP and ATP- $\gamma$ S. With the two ClpB sensor-1 mutants (T315A and T719A) and the two Walker B mutants (E279A and E678A), as the ratio of ATP- $\gamma$ S to ATP was increased, the rate of nucleotide hydrolysis slowed (Fig. 6a). Both ClpB(E279A) and ClpB(N719A) hydrolyzed ATP at a two-fold faster rate than did wild-type ClpB, for unknown reasons. With Hsp104 NBD-2 mutants (N728A and K620T), the ATPase activity was inhibited about 50% when the ATP/ATP- $\gamma$ S ratio was 3:1, in contrast to the lack of inhibition of the wild-type Hsp104 at this ratio of ATP to ATP- $\gamma$ S (Fig. 6c). With Hsp104(K620T), the rate of ATP hydrolysis was markedly faster than the wild-type rate. Thus, although there is not a simple correlation between the rates of ATP hydrolysis and the rates of remodeling, for both ClpB and Hsp104 mutants whose remodeling activities were inhibited by ATP- $\gamma$ S, their ATPase activities were similarly inhibited by ATP- $\gamma$ S.

### Effects of ATP and ATP- $\gamma$ S on prion remodeling by Hsp104

Finally, we examined how mixtures of ATP and ATP- $\gamma$ S affect Hsp104 remodeling reactions involving an unusual substrate that can exist stably in two different extremes of protein conformation. Hsp104 controls the inheritance of the yeast prion [PSI<sup>+</sup>], which consists of self-propagating amyloid fibers generated by the Sup35 protein's prion domain, NM<sup>11</sup>. In its prion state, NM adopts an extremely stable  $\beta$ -sheet-rich amyloid conformation<sup>40,41</sup>. At high concentrations, Hsp104 rapidly disassembled these unusually stable fibers in an ATP-dependent reaction (Fig. 7a). The disassembly reaction was not supported by ATP- $\gamma$ S alone, and mixtures of ATP and ATP- $\gamma$ S were inhibitory. Even an ATP/ATP- $\gamma$ S ratio of 6:1 inhibited fiber disassembly, and a 1:1 ratio abolished it (Fig. 7a). In keeping with these observations, neither Hsp104(N728A) nor Hsp104(K620T) are able to disassemble NM fibers<sup>26</sup> even though they can resolve small GFP aggregates (Fig. 4b). Thus, Hsp104 has an absolute requirement for ATP to remodel the stable conformation of NM fibers.

In the nonprion state, NM has the unusual capacity to populate a predominantly random-coil conformation for extended periods<sup>40</sup>. At low concentrations, Hsp104 catalyzed the folding of these largely unstructured proteins into the  $\beta$ -sheet-rich prion state in two ways (Fig. 7b,c). First, it promoted the formation of a crucial oligomeric intermediate of NM, detected using a conformation-specific antibody<sup>26</sup>, which is essential to nucleate amyloid assembly and eliminate the lag phase (the time before the first appearance of amyloid) (Fig. 7c). Second, it accelerated the assembly phase (the time between the first appearance of amyloid and the completion of assembly) by severing NM fibers to create additional polymerization surfaces for NM assembly<sup>26</sup> (Fig. 7b). The latter activity, like fiber disassembly, was supported by ATP but not ATP- $\gamma$ S (Fig. 7b). At all ratios of ATP to ATP- $\gamma$ S, the acceleration of assembly was inhibited (Fig. 7b). Thus, as

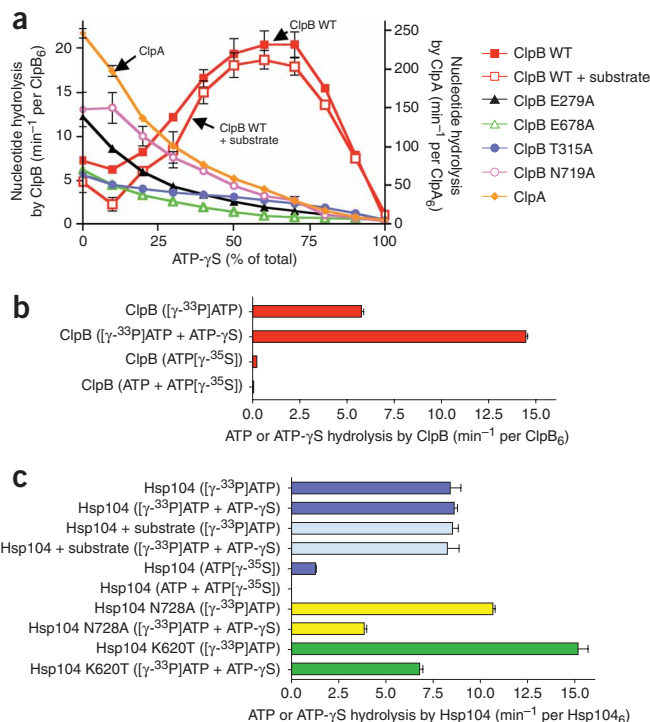


**Figure 6** Nucleotide hydrolysis by ClpB and Hsp104. (a) Nucleotide hydrolysis by ClpB, ClpB mutants and ClpA in the presence of the indicated amounts of ATP- $\gamma$ S. ClpB<sub>6</sub> denotes one ClpB hexamer. Substrate, RepA<sub>1-70</sub>-GFP. (b) ATP and ATP- $\gamma$ S hydrolysis by ClpB. (c) ATP and ATP- $\gamma$ S hydrolysis by Hsp104 and Hsp104 mutants. Hsp104<sub>6</sub> denotes one Hsp104 hexamer. In a–c, data are means  $\pm$  s.d. ( $n = 3$ ). WT, wild-type.

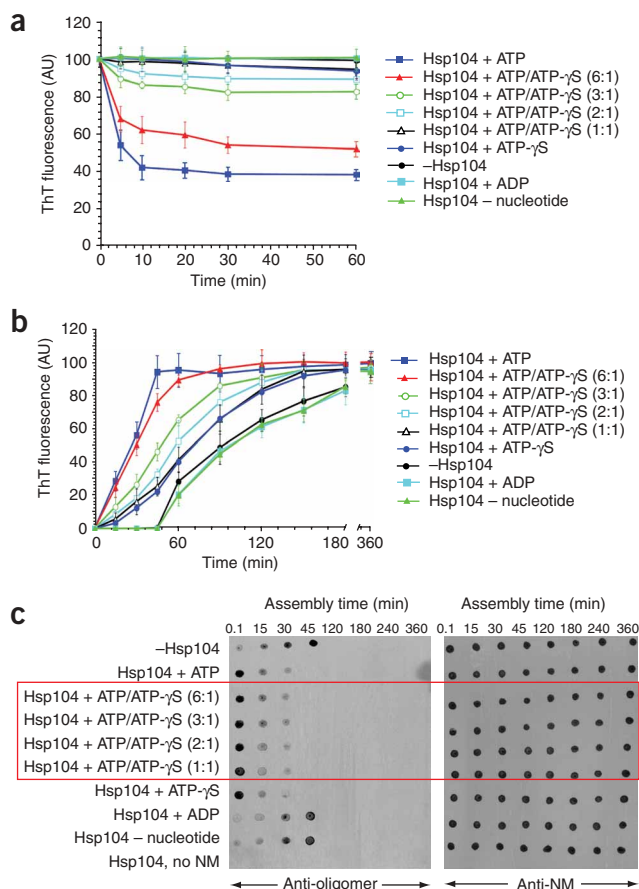
with fiber disassembly, the acceleration of the assembly phase by fiber severing is not stimulated by the mixture of ATP and ATP- $\gamma$ S, but rather is inhibited.

By contrast, Hsp104 eliminated the lag phase, by catalyzing the formation of the crucial oligomeric species that nucleate assembly, in the presence of ATP or ATP- $\gamma$ S but not in the presence of ADP or in the absence of nucleotide (Fig. 7b,c). Thus, ATP or ATP- $\gamma$ S binding promotes this prion-folding activity. This demonstrates the versatility of Hsp104 hexamers, in that they can promote protein folding or unfolding, depending on the reaction conditions and nature of the substrate.

## DISCUSSION

Our finding that a mixture of ATP and ATP- $\gamma$ S unleashes the protein-remodeling activities of ClpB and Hsp104 has led to unexpected insights into their reaction mechanisms. The use of ATP- $\gamma$ S allowed us to discover previously uncharacterized features of the ATPase domains that control their remodeling activities. For the first time, it allowed us to study ClpB and Hsp104 remodeling activities without the complicating effects of cochaperones and to do so with substrates that were tractable for dynamic analysis.

Researchers have examined the effects of ATP- $\gamma$ S on a large number of ATPases, with which it acts as a classic competitive inhibitor. To our knowledge, this is the first case in which ATP- $\gamma$ S stimulates a reaction requiring ATP hydrolysis. The absence of literature on activating effects of ATP and ATP- $\gamma$ S is not because the mixture has not been tested on other proteins. When we examined the effects of such mixtures on ClpA, another Hsp100 protein with two AAA+ domains



per monomer, its remodeling activities were not activated. Rather, ATP-γS inhibited remodeling. Thus, the unexpected effects of mixed nucleotides in unleashing the otherwise tightly restricted remodeling capacity of ClpB and Hsp104 reveals that there is something distinctive about their reaction cycle.

Using Hsp104 mutants in various Walker A and sensor-1 motifs, we discovered that remodeling can be triggered by impeding ATP hydrolysis at NBD-2. As there is known allosteric communication between the two NBDs<sup>19,20</sup>, it is likely that signals originating in the altered NBD-2 of the mutants are propagated through the coiled-coil middle domain to the distant functional NBD-1, resulting in a conformational state of the hexamer conducive for protein remodeling. In contrast to Hsp104, ClpB mutants with defective ATPase activity at either NBD-1 or NBD-2 could trigger protein-remodeling activity. This difference most likely reflects differences in the properties of NBD-1 and NBD-2 in the respective proteins that have accrued, perhaps as a consequence of genetic drift or selective pressures. What is most noteworthy is that protein remodeling by ClpB and Hsp104 is controlled by very similar mechanisms, yet is distinct from remodeling by ClpA.

Analyses of various nucleotide combinations revealed that ATPase activity must be asymmetrically decelerated in a specific manner to trigger ClpB and Hsp104 protein-remodeling activities. Only mixtures of ATP and ATP-γS could elicit the protein-remodeling activities. Mixtures of ATP and ADP or ATP and AMP-PNP did not promote remodeling, even though addition of ADP or AMP-PNP would also decelerate ATPase activity. In addition, slowing hydrolysis by limiting ATP did not elicit remodeling activities. These data imply that it is not simply slow hydrolysis that is essential to elicit the remodeling activity.

**Figure 7** Effects of ATP and ATP-γS on prion remodeling by Hsp104.

(a) Prion disassembly by Hsp104. ThT, thioflavin-T; AU, arbitrary units.

(b) Prion assembly in the presence of Hsp104. In **a** and **b**, values represent means  $\pm$  s.d. ( $n = 3$ ). (c) Prion assembly reactions in the presence of Hsp104, probed for the presence of either oligomer or NM.

This implication was clarified by the direct measurements of ATP hydrolysis. ATP-γS stimulated ATP hydrolysis by ClpB and did not inhibit ATP hydrolysis by Hsp104, whereas it inhibited hydrolysis by the ClpB and Hsp104 mutants. Together, these results suggest that the binding and/or slow hydrolysis of ATP-γS at a subset of the 12 nucleotide-binding sites actually translates, through interdomain communication, into increased ATP hydrolysis at other nucleotide-binding sites.

Why should there be a requirement for slow hydrolysis at one NBD to elicit remodeling activities, as demonstrated by the results with mutant proteins? We suggest that the multiple ATP-binding sites of the Hsp104 or ClpB hexamer must bind nucleotide, so that the ATP conformation is induced. In addition, ATP hydrolysis must be slow at NBD-2 of Hsp104 and at either NBD of ClpB to ensure that substrates are not prematurely released without unfolding, whereas hydrolysis at the other NBD must proceed at a rate sufficient to promote energy-dependent remodeling. Although it is difficult to compare AAA+ proteins with one AAA+ domain per monomer to those with two AAA+ domains per monomer, this need for holding and unfolding is slightly reminiscent of that proposed for ClpX. In ClpX, there is asymmetric nucleotide occupancy of the six ATP-binding sites in the single AAA+ domain<sup>42</sup>. For Hsp104 and ClpB, the mutants demonstrate that a balanced asymmetry between the two sets of AAA+ domains stimulates the remodeling activities.

This unexpected reaction mechanism may apply more broadly to other hexameric AAA+ ATPases with two AAA+ domains per monomer. For example, it would explain the otherwise puzzling finding that the NBD-2 of *N*-ethylmaleimide-sensitive fusion protein (NSF) has conserved nucleotide-binding activity but little or no ATPase activity<sup>43</sup>, yet is able to disassemble a large number of protein complexes involved in vesicle trafficking<sup>1</sup>. Similarly, NBD-1 of p97 is also catalytically inactive<sup>44</sup>, yet p97 assists the retrotranslocation of diverse polypeptides from the endoplasmic reticulum to the cytosol for proteasomal degradation<sup>1</sup>.

Because ATP-γS is a nonphysiological nucleotide, it is likely that other factors mimic the stimulatory effects of ATP-γS *in vivo*. ClpB and Hsp104 usually cooperate with Hsp70 and Hsp40 chaperones<sup>8–10</sup> as well as small Hsps<sup>28,45</sup>, in various disaggregation scenarios. Our results suggest that a major function of the cofactors is to coordinate the ATPase cycles of the two NBDs during substrate remodeling. Cochaperones might interact directly with ClpB or Hsp104 (refs. 8,19,46,47) in such a way that they attain an optimal mode of ATPase activity for protein disaggregation. Alternatively, initial remodeling of the aggregate surface by cochaperones<sup>17,31,48</sup> might ensure that the substrate itself effects the appropriate changes in ClpB or Hsp104 ATPase activity. In either way, cochaperones would directly or indirectly facilitate the asymmetric deceleration of ATPase activity at an NBD during the protein-remodeling process. Such tight regulation by Hsp70/DnaK or other cofactors would ensure successful deployment and activation of Hsp104 or ClpB remodeling activity, whenever or wherever it is needed most. However, although this putative role for Hsp70/DnaK may be crucial for maximal synergy between Hsp104 or ClpB and Hsp70/DnaK during disaggregation, Hsp70/DnaK must be doing more than simply coordinating the Hsp104 or ClpB ATPase cycle, as mutants that are



active in protein remodeling *in vitro* in the absence of cochaperones do not convey thermotolerance *in vivo*<sup>20,35,37</sup>. The Hsp70/DnaK system may also help present aggregated polypeptides to Hsp104/ClpB at an early stage of disaggregation<sup>8,17</sup>, and it undoubtedly helps newly solubilized polypeptides to refold once they are released from Hsp104 or ClpB<sup>8,9</sup>.

Notably, the asymmetric deceleration of ATPase activity by ATP- $\gamma$ S or point mutations cannot be tolerated for the remodeling of some substrates, as with the disassembly of Sup35 prions by Hsp104 (refs. 26,27). In these instances, the substrate may itself impose the requisite changes on Hsp104 ATPase activity. Alternatively, the remodeling of some substrates may require all protomers of the hexamer to bind and hydrolyze ATP in a sequential or concerted manner. This is in contrast to restricted probabilistic events where only select protomers hydrolyze ATP during substrate remodeling, which can be sufficient for many functions of another AAA+ ATPase, ClpX<sup>49</sup>. Indeed, in some situations, Hsp104 and ClpB hexamers may even need to switch between probabilistic and concerted modes of ATP hydrolysis. This may also explain why Hsp104 NBD-2 mutants and ClpB NBD-1 or NBD-2 mutants do not provide thermotolerance<sup>20,35,37</sup>. Alternatively, these mutants may be less able to collaborate productively or synergistically with cochaperones. We suggest that it is the versatility of reaction mechanisms that ClpB and Hsp104 hexamers can bring to bear on a wide variety of different substrates that guarantees successful reactivation of the entire aggregated proteome after environmental stress.

## METHODS

**Plasmids.** To generate a plasmid expressing ClpB, a *clpB* PCR product containing a 5' NdeI and a 3' EcoRI site was cut and ligated into NdeI- and EcoRI-digested pET24b (Novagen). Mutants were created by site-directed mutagenesis using the QuikChange kit (Stratagene).

**Proteins and DNA.** P1 RepA<sup>50</sup>, ClpA<sup>50</sup>, GFP<sup>51</sup>, RepA<sub>1-70</sub>-GFP<sup>51</sup>, GroEL<sub>trap</sub><sup>32</sup> (GroEL(D87K)), Hsp104 and Hsp104 mutants<sup>26</sup>, ClpB and ClpB mutants<sup>37</sup>, and [<sup>3</sup>H]*oriP1* DNA<sup>30</sup> (2,200 c.p.m. fmol<sup>-1</sup>) were prepared as described in references. Protein concentrations given are for monomeric GFP and RepA<sub>1-70</sub>-GFP, dimeric RepA, tetradecameric GroEL<sub>trap</sub> and hexameric ClpA, ClpB and Hsp104.

**Assays.** RepA activation assays (20  $\mu$ l) contained buffer A (20 mM Tris-HCl (pH 7.5), 100 mM KCl, 5 mM DTT, 0.1 mM EDTA, 10% (vol/vol) glycerol), 4 mM total nucleotide where indicated, 10 mM MgCl<sub>2</sub>, 50  $\mu$ g ml<sup>-1</sup> BSA, 0.005% (vol/vol) Triton X-100, 4 nM RepA and either 1  $\mu$ M ClpB or ClpB mutant, 1  $\mu$ M Hsp104 or Hsp104 mutant, or 30 nM ClpA, as indicated. When two nucleotides were added, the ratio of ATP to the second nucleotide was 1:1 for ClpB, ClpB mutants and ClpA, and 3:1 for Hsp104 and Hsp104 mutants. When the ratio of ATP to ATP- $\gamma$ S was varied with ClpB, 350 nM ClpB was used. After 10 min at 23 °C, 12 mM EDTA was added and reactions were chilled to 0 °C. Calf thymus DNA (1  $\mu$ g) and 13 fmol of [<sup>3</sup>H]*oriP1* plasmid DNA were added. After 5 min at 0 °C, the mixtures were filtered through nitrocellulose filters and retained radioactivity was measured.

GFP reactivation assays (100  $\mu$ l) contained buffer A, 4 mM total nucleotide where indicated, an ATP-regenerating system (ARS; 20 mM creatine phosphate and 6  $\mu$ g creatine kinase), 20 mM MgCl<sub>2</sub>, 0.45  $\mu$ M heat-aggregated GFP (heated 10 min at 80 °C at 4.5  $\mu$ M and then diluted) and 1  $\mu$ M of either ClpB, Hsp104 or ClpA, as indicated. When two nucleotides were added, the ratio of ATP to the second nucleotide was 1:1 for ClpB, ClpB mutants and ClpA, and 3:1 for Hsp104 and Hsp104 mutants. When the ARS was omitted, 5 units hexokinase and 5 mM glucose were added. Where indicated, 2.5  $\mu$ M GroEL<sub>trap</sub> was added. Reactivation was monitored over time at 23 °C using a Perkin-Elmer LS50B luminescence spectrophotometer with a well plate reader. Excitation and emission wavelengths were 395 nm and 510 nm, respectively.

Unfolding assays (100  $\mu$ l) contained buffer A, 20  $\mu$ g ml<sup>-1</sup> BSA, 0.005% (vol/vol) Triton X-100, 20 mM creatine phosphate, 6  $\mu$ g creatine kinase, 10 mM MgCl<sub>2</sub>, 4 mM nucleotide as indicated, 0.7  $\mu$ M RepA<sub>1-70</sub>-GFP, and 2.1  $\mu$ M ClpB, ClpB mutants, Hsp104, Hsp104 mutants or ClpA, as indicated. GroEL<sub>trap</sub> (2.5  $\mu$ M) was added where indicated. When two nucleotides were added, the ratio of ATP to the second nucleotide was 1:1 for ClpB, ClpB mutants and ClpA, and 3:1 for Hsp104 and Hsp104 mutants. When the ARS was omitted, 5 units hexokinase and 5 mM glucose were added. Fluorescence was monitored as above.

Steady-state unfolding assays were done like the unfolding assays described above, but with 1 mM ATP and 1 mM ATP- $\gamma$ S. After 10 min of incubation, one of the following was added: 10 mM ATP, 10 mM ATP with GroEL<sub>trap</sub>, 10 mM ADP, 10 mM ADP with GroEL<sub>trap</sub>, 10 mM ATP- $\gamma$ S, or GroEL<sub>trap</sub> alone.

ATPase assays (25  $\mu$ l) contained buffer A, 0.005% (vol/vol) Triton X-100, 4 mM total nucleotide where indicated, 20 mM MgCl<sub>2</sub>, 0.4  $\mu$ M RepA<sub>1-70</sub>-GFP where indicated, and 2  $\mu$ M of either ClpB, ClpB mutant, Hsp104, Hsp104 mutant or ClpA, as indicated. When ATP and ATP- $\gamma$ S were used, the ratio was 1:1 for ClpB, ClpB mutants and ClpA, 3:1 for Hsp104 and Hsp104 mutants, or varied as indicated. For the assays containing nonradioactive nucleotides, phosphate production was determined using a malachite green phosphate detection kit (BioMol). For the radioactivity assays, 1  $\mu$ Ci of [ $\gamma$ -<sup>35</sup>S]ATP (>1,000 Ci mM<sup>-1</sup>; GE Healthcare) or 0.1  $\mu$ Ci of [ $\gamma$ -<sup>33</sup>P]ATP (>3,000 Ci mM<sup>-1</sup>; GE Healthcare) was used. Reaction mixtures with radioactive ATP or ATP- $\gamma$ S were incubated 15 min or 90 min at 23 °C, respectively. Those with [ $\gamma$ -<sup>33</sup>P]ATP were analyzed as described<sup>52</sup>. Those with [ $\gamma$ -<sup>35</sup>S]ATP were stopped with the addition of 37 mM EDTA; aliquots (5  $\mu$ l) were spotted on polyethyleneimine thin-layer plates, developed in 0.5 M formic acid and 0.5 M LiCl, air-dried and analyzed using a phosphorimaging device.

Prion assembly and disassembly assays were done as described<sup>26</sup>. For disassembly, 2.5  $\mu$ M NM was incubated for 6 h with rotation (80 r.p.m.) to generate prions and then incubated with 0.3  $\mu$ M Hsp104 at 25 °C and 5 mM total nucleotide as indicated. Where indicated, the ratio of ATP to ATP- $\gamma$ S was varied. Disassembly was monitored by thioflavin-T fluorescence. To measure assembly, 2.5  $\mu$ M unseeded, rotated (80 r.p.m.) NM was incubated with 0.03  $\mu$ M Hsp104 plus 5 mM total nucleotide as indicated, using the ATP/ATP- $\gamma$ S ratios indicated. Prion assembly was monitored by thioflavin-T fluorescence. At various times during the assembly reaction, samples were applied to nitrocellulose and probed with antibody to the oligomer (see Acknowledgments)<sup>26</sup> or to NM<sup>26</sup>.

## ACKNOWLEDGMENTS

This research was supported by the Intramural Research Program of the NIH, National Cancer Institute, Center for Cancer Research, an American Heart Association scientist development grant to J.S. and NIH grants to M.Z. (GM58626) and S.L. (GM25874). We thank C. Glabe (University of California, Irvine) for the antibody to oligomer and K. Mizuuchi and K. McKenney for helpful discussions.

## AUTHOR CONTRIBUTIONS

S.M.D., J.S. and J.R.H. designed experiments, performed experiments, interpreted data and wrote the manuscript; M.Z., S.L. and S.W. designed experiments, interpreted data and wrote the manuscript.

## COMPETING INTERESTS STATEMENT

The authors declare that they have no competing financial interests.

Published online at <http://www.nature.com/nsmb/>

Reprints and permissions information is available online at <http://npg.nature.com/reprintsandpermissions>

- Hanson, P.I. & Whiteheart, S.W. AAA+ proteins: have engine, will work. *Nat. Rev. Mol. Cell Biol.* **6**, 519–529 (2005).
- Erzberger, J.P. & Berger, J.M. Evolutionary relationships and structural mechanisms of AAA+ proteins. *Annu. Rev. Biophys. Biomol. Struct.* **35**, 93–114 (2006).
- Hedges, S.B., Blair, J.E., Venturi, M.L. & Shoe, J.L. A molecular timescale of eukaryote evolution and the rise of complex multicellular life. *BMC Evol. Biol.* **4**, 2 (2004).
- Sanchez, Y. & Lindquist, S.L. HSP104 required for induced thermotolerance. *Science* **248**, 1112–1115 (1990).
- Squires, C.L., Pedersen, S., Ross, B.M. & Squires, C. ClpB is the *Escherichia coli* heat shock protein F84.1. *J. Bacteriol.* **173**, 4254–4262 (1991).



6. Sanchez, Y., Taulien, J., Borkovich, K.A. & Lindquist, S. Hsp104 is required for tolerance to many forms of stress. *EMBO J.* **11**, 2357–2364 (1992).
7. Parsell, D.A., Kowal, A.S., Singer, M.A. & Lindquist, S. Protein disaggregation mediated by heat-shock protein Hsp104. *Nature* **372**, 475–478 (1994).
8. Glover, J.R. & Lindquist, S. Hsp104, Hsp70, and Hsp40: a novel chaperone system that rescues previously aggregated proteins. *Cell* **94**, 73–82 (1998).
9. Goloubinoff, P., Mogk, A., Zvi, A.P., Tomoyasu, T. & Bukau, B. Sequential mechanism of solubilization and refolding of stable protein aggregates by a bichaperone network. *Proc. Natl. Acad. Sci. USA* **96**, 13732–13737 (1999).
10. Zolkiewski, M. ClpB cooperates with DnaK, DnaJ, and GrpE in suppressing protein aggregation. A novel multi-chaperone system from *Escherichia coli*. *J. Biol. Chem.* **274**, 28083–28086 (1999).
11. Shorter, J. & Lindquist, S. Prions as adaptive conduits of memory and inheritance. *Nat. Rev. Genet.* **6**, 435–450 (2005).
12. Lee, S. *et al.* The structure of ClpB: a molecular chaperone that rescues proteins from an aggregated state. *Cell* **115**, 229–240 (2003).
13. Parsell, D.A., Kowal, A.S. & Lindquist, S. *Saccharomyces cerevisiae* Hsp104 protein. Purification and characterization of ATP-induced structural changes. *J. Biol. Chem.* **269**, 4480–4487 (1994).
14. Akoev, V., Gogol, E.P., Barnett, M.E. & Zolkiewski, M. Nucleotide-induced switch in oligomerization of the AAA+ ATPase ClpB. *Protein Sci.* **13**, 567–574 (2004).
15. Lum, R., Tkach, J.M., Vierling, E. & Glover, J.R. Evidence for an unfolding/threading mechanism for protein disaggregation by *Saccharomyces cerevisiae* Hsp104. *J. Biol. Chem.* **279**, 29139–29146 (2004).
16. Schlieker, C. *et al.* Substrate recognition by the AAA+ chaperone ClpB. *Nat. Struct. Mol. Biol.* **11**, 607–615 (2004).
17. Weibezahn, J. *et al.* Thermotolerance requires refolding of aggregated proteins by substrate translocation through the central pore of ClpB. *Cell* **119**, 653–665 (2004).
18. Barnett, M.E., Nagy, M., Kedzierska, S. & Zolkiewski, M. The amino-terminal domain of ClpB supports binding to strongly aggregated proteins. *J. Biol. Chem.* **280**, 34940–34945 (2005).
19. Cashikar, A.G. *et al.* Defining a pathway of communication from the C-terminal peptide binding domain to the N-terminal ATPase domain in a AAA protein. *Mol. Cell* **9**, 751–760 (2002).
20. Hattendorf, D.A. & Lindquist, S.L. Cooperative kinetics of both Hsp104 ATPase domains and interdomain communication revealed by AAA sensor-1 mutants. *EMBO J.* **21**, 12–21 (2002).
21. Mogk, A. *et al.* Roles of individual domains and conserved motifs of the AAA+ chaperone ClpB in oligomerization, ATP hydrolysis, and chaperone activity. *J. Biol. Chem.* **278**, 17615–17624 (2003).
22. Schirmer, E.C., Ware, D.M., Queitsch, C., Kowal, A.S. & Lindquist, S.L. Subunit interactions influence the biochemical and biological properties of Hsp104. *Proc. Natl. Acad. Sci. USA* **98**, 914–919 (2001).
23. Schlee, S., Groemping, Y., Herde, P., Seidel, R. & Reinstein, J. The chaperone function of ClpB from *Thermus thermophilus* depends on allosteric interactions of its two ATP-binding sites. *J. Mol. Biol.* **306**, 889–899 (2001).
24. Shorter, J. & Lindquist, S. Navigating the ClpB channel to solution. *Nat. Struct. Mol. Biol.* **12**, 4–6 (2005).
25. Schirmer, E.C., Homann, O.R., Kowal, A.S. & Lindquist, S. Dominant gain-of-function mutations in Hsp104p reveal crucial roles for the middle region. *Mol. Biol. Cell* **15**, 2061–2072 (2004).
26. Shorter, J. & Lindquist, S. Hsp104 catalyzes formation and elimination of self-replicating Sup35 prion conformers. *Science* **304**, 1793–1797 (2004).
27. Shorter, J. & Lindquist, S. Destruction or potentiation of different prions catalyzed by similar hsp104 remodeling activities. *Mol. Cell* **23**, 425–438 (2006).
28. Haslbeck, M., Miess, A., Stromer, T., Walter, S. & Buchner, J. Disassembling protein aggregates in the yeast cytosol. The cooperation of Hsp26 with Ssa1 and Hsp104. *J. Biol. Chem.* **280**, 23861–23868 (2005).
29. Wickner, S. *et al.* A molecular chaperone, ClpA, functions like DnaK and DnaJ. *Proc. Natl. Acad. Sci. USA* **91**, 12218–12222 (1994).
30. Wickner, S., Hoskins, J. & McKenney, K. Function of DnaJ and DnaK as chaperones in origin-specific DNA binding by RepA. *Nature* **350**, 165–167 (1991).
31. Zietkiewicz, S., Lewandowska, A., Stocki, P. & Liberek, K. Hsp70 chaperone machine remodels protein aggregates at the initial step of Hsp70-Hsp100-dependent disaggregation. *J. Biol. Chem.* **281**, 7022–7029 (2006).
32. Weber-Ban, E.U., Reid, B.G., Miranker, A.D. & Horwich, A.L. Global unfolding of a substrate protein by the Hsp100 chaperone ClpA. *Nature* **401**, 90–93 (1999).
33. Martin, J. *et al.* Chaperonin-mediated protein folding at the surface of groEL through a 'molten globule'-like intermediate. *Nature* **352**, 36–42 (1991).
34. Dietz, H. & Rief, M. Exploring the energy landscape of GFP by single-molecule mechanical experiments. *Proc. Natl. Acad. Sci. USA* **101**, 16192–16197 (2004).
35. Parsell, D.A., Sanchez, Y., Stitzel, J.D. & Lindquist, S. Hsp104 is a highly conserved protein with two essential nucleotide-binding sites. *Nature* **353**, 270–273 (1991).
36. Schirmer, E.C., Queitsch, C., Kowal, A.S., Parsell, D.A. & Lindquist, S. The ATPase activity of Hsp104, effects of environmental conditions and mutations. *J. Biol. Chem.* **273**, 15546–15552 (1998).
37. Barnett, M.E. & Zolkiewski, M. Site-directed mutagenesis of conserved charged amino acid residues in ClpB from *Escherichia coli*. *Biochemistry* **41**, 11277–11283 (2002).
38. Watanabe, Y.H., Motohashi, K. & Yoshida, M. Roles of the two ATP binding sites of ClpB from *Thermus thermophilus*. *J. Biol. Chem.* **277**, 5804–5809 (2002).
39. Weibezahn, J., Schlieker, C., Bukau, B. & Mogk, A. Characterization of a trap mutant of the AAA+ chaperone ClpB. *J. Biol. Chem.* **278**, 32608–32617 (2003).
40. Scheibel, T. & Lindquist, S.L. The role of conformational flexibility in prion propagation and maintenance for Sup35p. *Nat. Struct. Mol. Biol.* **8**, 958–962 (2001).
41. Scheibel, T. *et al.* Conducting nanowires built by controlled self-assembly of amyloid fibers and selective metal deposition. *Proc. Natl. Acad. Sci. USA* **100**, 4527–4532 (2003).
42. Hersch, G.L., Burton, R.E., Bolon, D.N., Baker, T.A. & Sauer, R.T. Asymmetric interactions of ATP with the AAA+ ClpX<sub>6</sub> unfoldase: allosteric control of a protein machine. *Cell* **121**, 1017–1027 (2005).
43. Whiteheart, S.W. *et al.* N-ethylmaleimide-sensitive fusion protein: a trimeric ATPase whose hydrolysis of ATP is required for membrane fusion. *J. Cell Biol.* **126**, 945–954 (1994).
44. Wang, Q., Song, C. & Li, C.C. Molecular perspectives on p97-VCP: progress in understanding its structure and diverse biological functions. *J. Struct. Biol.* **146**, 44–57 (2004).
45. Mogk, A. *et al.* Refolding of substrates bound to small Hsps relies on a disaggregation reaction mediated most efficiently by ClpB/DnaK. *J. Biol. Chem.* **278**, 31033–31042 (2003).
46. Schlee, S., Beinker, P., Akhrymuk, A. & Reinstein, J. A chaperone network for the resolubilization of protein aggregates: direct interaction of ClpB and DnaK. *J. Mol. Biol.* **336**, 275–285 (2004).
47. Kedzierska, S., Chesnokova, L.S., Witt, S.N. & Zolkiewski, M. Interactions within the ClpB/DnaK bi-chaperone system from *Escherichia coli*. *Arch. Biochem. Biophys.* **444**, 61–65 (2005).
48. Zietkiewicz, S., Krzewska, J. & Liberek, K. Successive and synergistic action of the Hsp70 and Hsp100 chaperones in protein disaggregation. *J. Biol. Chem.* **279**, 44376–44383 (2004).
49. Martin, A., Baker, T.A. & Sauer, R.T. Rebuilt AAA + motors reveal operating principles for ATP-fuelled machines. *Nature* **437**, 1115–1120 (2005).
50. Hoskins, J.R. & Wickner, S. Two peptide sequences can function cooperatively to facilitate binding and unfolding by ClpA and degradation by ClpAP. *Proc. Natl. Acad. Sci. USA* **103**, 909–914 (2006).
51. Hoskins, J.R., Kim, S.Y. & Wickner, S. Substrate recognition by the ClpA chaperone component of ClpAP protease. *J. Biol. Chem.* **275**, 35361–35367 (2000).
52. Shacter, E. Organic extraction of Pi with isobutanol/toluene. *Anal. Biochem.* **138**, 416–420 (1984).
53. Schwede, T., Kopp, J., Guex, N. & Peitsch, M.C. SWISS-MODEL: an automated protein homology-modeling server. *Nucleic Acids Res.* **31**, 3381–3385 (2003).